Organic & Biomolecular Chemistry

Dynamic Article Links

Cite this: *Org. Biomol. Chem.*, 2011, **9**, 7763

www.rsc.org/obc

PAPER

8-(*p*-CF_3-cinnamyl)-modified purine nucleosides as promising fluorescent probes†

Lital Zilbershtein, Alon Silberman and Bilha Fischer*

Received 1st May 2011, Accepted 19th July 2011
DOI: 10.1039/c1ob05681f

Natural nucleotides are not useful as fluorescent probes because of their low quantum yields. Therefore, a common methodology for the detection of RNA and DNA is the application of extrinsic fluorescent dyes coupled to bases in oligonucleotides. To overcome the many limitations from which fluorescent nucleotide–dye conjugates suffer, we have developed novel purine nucleosides with intrinsic fluorescence to be incorporated into oligonucleotide probes. For this purpose we synthesized adenosine and guanosine fluorescent analogues **7–25**, conjugated at the C8 position with aryl/heteroaryl moieties either directly, or *via* alkenyl/alkynyl linkers. Directly conjugated analogues **7–14**, exhibited high quantum yields, ϕ >0.1, and short λ_{em} (<385 nm). Alkynyl conjugated analogues **22–25**, exhibited low quantum yields, ϕ <0.075, and λ_{em}<385 nm. The alkenyl conjugated analogues **15–21**, exhibited λ_{em} 408–459 nm. While analogues **15,16**, and **20** bearing an EDG on the aryl moiety, exhibited ϕ <0.02, analogues **17**, and **21** with EWG on the aryl moiety, exhibited extremely high quantum yields, $\phi \approx 0.8$, suggesting better intramolecular charge transfer. We determined the conformation of selected adenosine analogues. Directly conjugated analogue **8** and alkynyl conjugated analogue **22**, adapted the *syn* conformation, whereas alkenyl conjugated analogue **15** adapted the *anti* conformation. Based on the long emission wavelengths, high quantum yields, *anti* conformation and base-paring compatibility, we suggest analogues **17** and **21** for further development as fluorescent probes for the sensitive detection of genetic material.

Introduction

Previously, the detection of nucleic acids was based on radioactive labeling of nucleic acid probes (*e.g.* by ^{32}P).[1] This labeling allowed for instance, the detection of specific mRNA sequences.[2,3] However, these radioactive labeled probes suffer from fundamental disadvantages: they are hazardous, have short half-lives, and have limited signal emission. In contrast, fluorescent probes do not suffer from these disadvantages and have largely taken over as sensitive labels for identification and quantification of nucleic acids.[4]

The natural bases of nucleic acids are not useful as fluorescent probes because of their extremely low quantum yields.[5,6] Therefore, the use of extrinsic probes, namely, fluorescent dyes, is necessary. Currently marketed dyes for nucleic-acid staining and labeling include: intercalating dyes that are incorporated non-covalently to double stranded nucleic acids; minor groove-binding dyes; a dye-labeled streptavidin to detect a biotinylated probe, and large fluorescent dyes (*e.g.*, rhodamine, fluorescein, and Cy5/Cy3) that are incorporated covalently to oligonucleotides at positions that do not interfere with base pairing.[7] The latter have been applied to DNA microarray technology.[8] This technology involves covalent conjugation of nucleotides with large fluorescent dyes followed by enzymatic incorporation, resulting in a cDNA hybridization-capable probe. However, a large dye attached to a nucleotide alters the efficiency of enzymatic incorporation. The synthesis of long DNA/RNA probes is therefore unreliable and variation of fluorescence yield with degree of dye conjugation to the nucleic acid probe can significantly reduce the reliability of quantitative measures of hybridization-based assays.

Other currently used conjugated-dye technologies include Fluorescent *In Situ* Hybridization (FISH)[9] and Molecular Beacons (MB).[10–12] FISH probes are prepared from amino-allyl modified bases[13] used to allow the chemical synthesis of multiply-labeled fluorescent oligomer hybridization probes[14] in a two-step protocol involving first the incorporation of a slightly modified nucleotide into nucleic acid, followed by covalent binding of the fluorophore of interest (*e.g.* FITC, Cy3, Alexa-488). However, labeling with these fluorophores requires additional conjugation and purification steps following probe synthesis. Furthermore, the detection of endogenous levels of mRNA is difficult due to fluorescent background, and typically requires the generation of several probe sequences to the same mRNA resulting in signal enhancement.

To overcome many of the limitations of the above mentioned fluorescent probes, intrinsically fluorescent nucleosides

Department of Chemistry, Gonda-Goldschmied Medical Research Center, Bar-Ilan University, Ramat-Gan, 52900, Israel. E-mail: bilha.fischer@biu.ac.il; Fax: +972-3-6354907; Tel: +972-3-5318303

† Electronic supplementary information (ESI) available: ^{13}C and ^{1}H NMR spectra of reported compounds. See DOI: 10.1039/c1ob05681f

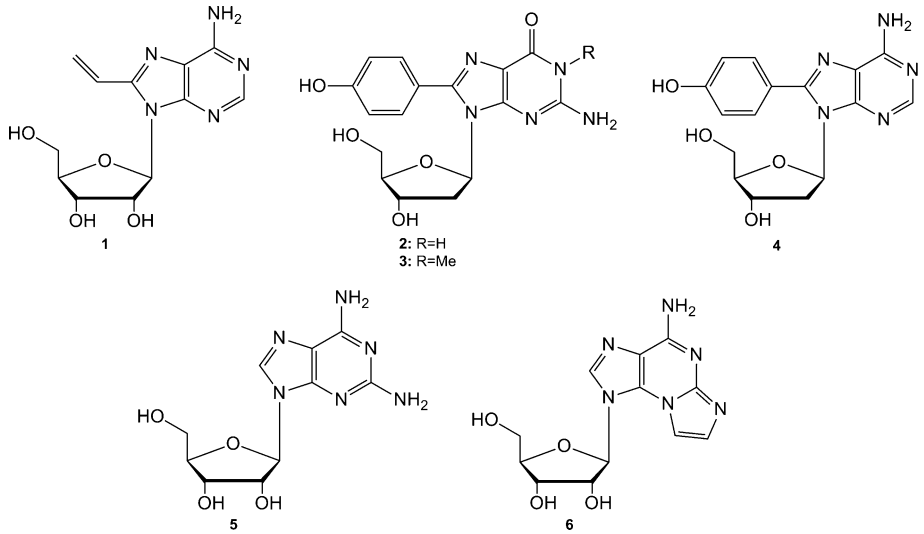

Fig. 1 Fluorescent purine nucleoside analogues: C8 extended adenosine analogues, **1–4**; 2-amino adenosine, **5**; N^2,N3-etheno-adenosine, **6**.

were introduced for numerous applications.[15] These nucleosides are minimally modified, at the nucleobase positions that do not interfere with base pairing, thus extending the nucleoside's fluorophore.

For example, extending the purine π system by C8 modifications, *e.g.* 8-vinyladenosine, **1** (Fig. 1) results in a longer emission wavelength and higher quantum yield as compared to adenosine (λ_{em} 388 nm; ϕ 0.66 *vs.* λ_{em} 319 nm; ϕ 0.00026).[16–18]

The purine π-system was also extended upon conjugation with aromatic moieties. Specifically, 8-(*p*-hydroxy-phenyl) nucleosides, **2–4** emit at ~390 nm with high quantum yields ranging from 0.25 to 0.56 in aqueous solution (pH 7).

2-Amino adenosine, **5**, has been employed in studies of nucleic acid structure and dynamics, due to the significant change of its quantum yield upon incorporation into single and double-strand oligonucleotides as compared to that of the monomer in water (ϕ 0.65).[19]

Previously, we have extended the adenine chromophore at C2,N3-positions to give N^2,N3-etheno-adenosine, **6**, as a novel probe exhibiting improved fluorescence characteristics (λ_{em} 420 nm; ϕ 0.03).[20]

The limitations of fluorescent dyes used in current hybridization-based technologies have encouraged us to develop novel intrinsically fluorescent adenine and guanine nucleosides that will be later incorporated into oligonucleotides. These probes include a minimal extension at the C8-position of adenosine (A) or guanosine (G), rather than attachment of large hydrophobic dyes to the nucleobase. In addition, A- and G- fluorescent nucleosides proposed here were designed to satisfy the following requirements: relatively long absorption and emission wavelengths, satisfactory quantum yield, and base-pairing compatibility. Specifically, long absorption and emission wavelengths (>450 nm), as well as satisfactory quantum yield (>0.1) are required to overcome auto-fluorescence of many cellular components excited by UV–vis radiation of suitable wavelengths (from 300 nm for aromatic amino acids to 550 nm for riboflavin). In addition, we extended A and G at the C8 position, which is not involved in base pairing, to obtain hybridization-compatible probes upon incorporation into oligonucleotides.

Here, we report on the design, synthesis, and spectral characterization of a series of C8-aryl/hetero-aryl conjugated adenosine and guanosine analogues **7–25** (Fig. 2). Moreover, we propose a mechanism for the analogues' fluorescence. In addition, we report on the compatibility of selected analogues for B-DNA formation based on their conformational analysis. This SAR study resulted in the identification of highly promising probes **17** (λ_{em} 439 nm; ϕ 0.81), and **21** (λ_{em} 459 nm; ϕ 0.80) suitable for hybridization assays upon incorporation in oligonucleotides.

Results

Design of intrinsically fluorescent A and G analogues

We designed novel C8 extended adenine and guanine nucleosides **7–25** as potential intrinsically fluorescent probes that are hybridization compatible. Extension of a purine nucleoside at C8 position was expected to result in longer excitation and emission wavelengths, and higher quantum yield, as compared to the parent compound.[21]

Here, we targeted a minimal modification of the nucleoside π-system with small aromatic/hetero-aromatic moieties. We conjugated these moieties to the purine ring *via* an alkenyl or alkynyl linker, or no linker at all, to study the effect of the linker on fluorescence.

Fluorescent A or G analogues **7–25** were designed as push–pull probes to enhance the fluorescent properties of purine nucleosides. Push–pull molecules are generally composed of three moieties: an electron donor (D, an electron rich aryl group); an electron acceptor (A, an electron poor aryl moiety), and an electron rich linker which is a double/triple bond (analogues **15–25**), or a single bond (analogues **7–14**). Since the electron-donating or -accepting character of A or G in push–pull molecules is relative to the other moiety, we explored the properties of both electron rich aryl groups (analogues **8–11, 15–16, 20** and **22–25**) and electron poor groups (analogues **17–19** and **21**) attached to either A or G.

Likewise, we investigated the effect of the number (1–3) and positions (*p*, *m*) of EDGs on the probe's fluorescence. The effect of the nucleobase (*i.e.*, adenine *vs.* guanine) on fluorescence was evaluated as well.

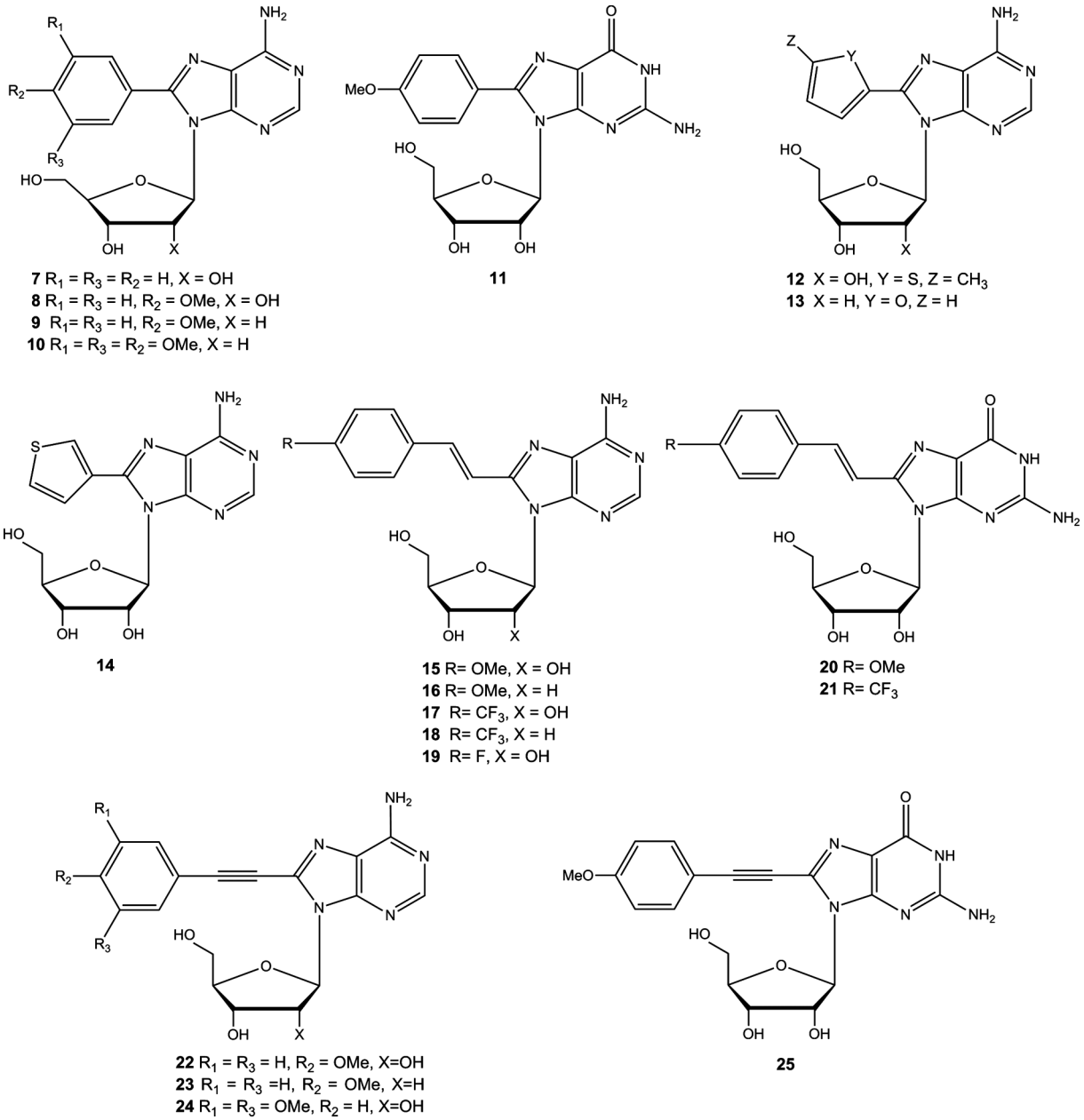

Fig. 2 Adenosine and guanosine analogues synthesized and studied here.

Synthesis of fluorescent nucleoside probes 7–25

We have applied the Suzuki–Miyuara coupling[22,23] for the preparation of analogues **7–21**, and the Sonogashira coupling[24,25] for the preparation of analogues **22–25**. The great advantage of these procedures is that no protecting groups are needed, thus allowing a single step reaction towards the desired conjugated nucleoside analogues.

Specifically, A and G were directly conjugated with aryl/heterocyclic boronic acids in the presence of Na_2CO_3 and a water-soluble catalytic system consisting of $Pd(OAc)_2$: P(*m*-$C_6H_4SO_3Na)_3$, in water–acetonitrile (2 : 1) at ~100 °C.[22,23] Products **7–10** and **12–14** were obtained in 13%–89% yield upon silica gel chromatography. To separate 8-(4-methoxyphenyl)-guanosine, **11**, from guanosine palladium complexes formed under the reaction's basic conditions,[26] the crude reaction residue was washed with boiling water. All salts and any unreacted 8-Br-G were removed by this procedure. The solid residue was then washed with EtOAc and Et_2O to remove any palladium complexes and traces of boronic acid, thus providing a highly pure product **11** in 21% yield.

Analogues **15, 16** and **20** were prepared from (*E*)-4-methoxystyrylboronic acid and 8-Br-A, 8-Br-dA, and 8-Br-G under Suzuki coupling conditions. The pure products were typically obtained from the reaction mixture as follows: analogue **15** was precipitated upon neutralization of the reaction mixture by 10% aqueous HCl, vacuum filtered and purified by excessive washing with H_2O and ACN resulting in pure **15** in 42% yield. However, analogues **16** and **20** were purified on a silica gel column and obtained in 83% and 10% yield, respectively. The low yield obtained for products **11** and **20**

Table 1 Spectral properties of analogues **7–25** measured in MeOH

Analogue	λ_{ab} (nm)	λ_{em} (nm)	ϕ	Standard
Adenine[17a]	361	319	0.00026	—
Guanine[17a]	275	303	0.0003	—
7	284	365, 387	0.11	tryptophan
8	284	361, 382	0.105	tryptophan
9	288	362, 381	0.46	tryptophan
10	292	365, 385	0.113	tryptophan
11	290	362, 383	0.23	tryptophan
12	309	354	0.054	quinine sulfate
13	306	360, 381	0.46	quinine sulfate
14	285	358, 382	0.21	tryptophan
15	345	394, 419	0.005	quinine sulfate
16	340	408	0.0025	quinine sulfate
17	340	439	0.81	quinine sulfate
18	338	438	0.74	quinine sulfate
19	333	436	0.025	quinine sulfate
20	350	430	0.018	quinine sulfate
21	357	459	0.80	quinine sulfate
22	323	355, 367, 382	0.05	quinine sulfate
23	323	355, 368, 384	0.062	tryptophan
24	316	365, 385	0.075	quinine sulfate
25	299	316, 330, 344	0.054	tryptophan

[a] Fluorescence data were obtained at room temperature in neutral aqueous solutions.

is due to the reduced reactivity of 8-bromoguanosine in the Suzuki–Miyaura reaction.[26] Analogues **17, 18** and **21**, prepared from (*E*)-[4-(trifluoromethyl)phenyl]vinylboronic acid and 8-Br-A, 8-Br-dA, and 8-Br-G, and analogue **19** prepared from (*E*)-(4-fluorophenyl)vinylboronic acid and 8-Br-A, were purified on a silica gel column and obtained in 40–73% yield.

The analogues bearing an alkynyl linker, **22–25**, were prepared by conjugation of 8-Br-A, 8-Br-dA, and 8-Br-G with 4-methoxyphenyl-ethynyl or 3,5-dimethoxyphenyl-ethynyl (with 8-Br-A). Specifically, the reactions were carried out in DMF at room temperature for 18 h (products **22–24**), or at 50 °C for 24 h (product **25**), in the presence of Et_3N and a catalytic system consisting of $Pd(Ph_3P)_4$/CuI. Purification of analogues **22–24** was achieved by chromatography on a silica gel column, resulting in products **22–24** in 26–95% yield. However, purification of the corresponding 8-((4-methoxyphenyl)ethynyl)-guanosine, **25**, was achieved as described above for **11**, resulting in only 15% yield. Here again, the reduced reactivity of 8-bromoguanosine in palladium catalyzed cross-coupling reactions resulted in a low yield of analogue **25**.

Spectral properties of analogues 7–25

The absorption and emission spectra of compounds **7–25** were measured in methanol, and the fluorescence quantum yields were determined compared to known standards such as tryptophan in H_2O (λ_{ex} 286 nm, λ_{em} 355 nm, ϕ 0.13) or quinine sulfate in 0.1 M H_2SO_4, (λ_{ex} 350 nm, λ_{em} 446 nm, ϕ 0.54)[27,28] (Table 1).

We have observed more than one emission band in the emission spectra of analogues **7–11, 13–15**, and **22–25** (a representative spectrum of analogue **13** is shown in Fig. 3). This phenomenon occurs due to vibrational progressions, explained by the Franck–Condon principle. The electron radiates back from different vibrational states in the first excited singlet state S_1 to different vibrational states on the ground state S_0, resulting in more than one emission wavelength, where the energy difference between the emission wavelengths is between 1000–2000 cm^{-1}.[29–31] In these

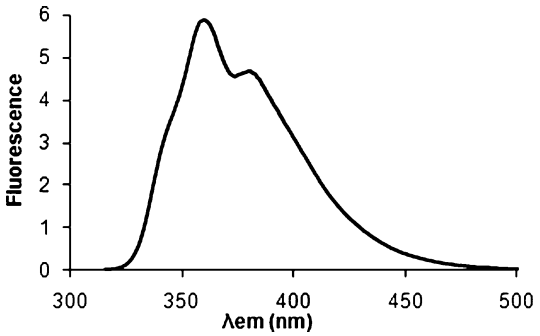

Fig. 3 A representative emission spectrum of analogue **13**.

cases, quantum yield calculations are based on the area under all emission bands. The energy difference between the spectral lines, of all above mentioned analogues, was 1000–2000 cm^{-1}, and was therefore considered to be due to a vibrational progression rather than an additional fluorescence band due to contamination.

We evaluated the dependence of probe fluorescence on the following parameters: type of linker, presence of an ED or an EW substituent on the aryl moiety, number of ED substituents, aryl *vs.* heteroaryl substituents, and type of nucleobase.

Type of linker. The effect of the linker between the nucleobase and the aryl group on fluorescence of A and G analogues was evaluated. Three types of linkers were compared: analogues **8** and **11**, 8-(4-methoxy-phenyl)-A and -G, analogues in which the aromatic moiety is directly coupled to the A/G C8-position, analogues **15** and **20**, 8-(2-(4-methoxyphenyl)-ethenyl)-A and -G, analogues in which the aromatic moiety is coupled to the A/G C8-position *via* an alkenyl linker, and analogues **22** and **25**, 8-(2-(4-methoxyphenyl)-ethynyl)-A and -G, analogues in which the aromatic moiety is conjugated to the A/G C8-position *via* an alkynyl linker. The analogues in which the aromatic moiety was directly coupled to the nucleobase **8** and **11**, exhibited relatively high quantum yields, ϕ 0.105 and 0.23, respectively, but short emission wavelengths ~360 and 380 nm. The analogues with the alkenyl linker, **15** and **20**, exhibited the lowest quantum yields ϕ 0.005 and 0.018, respectively, but, λ_{em} >400 nm. The analogues with the alkynyl linker, **22** and **25**, exhibited low quantum yields, ϕ 0.05 and 0.054 respectively, and emission wavelengths of 355, 367, 382 nm for analogue **22**, and 316, 330, 344 nm for analogue **25**, which were the shortest emission wavelengths.

Type of substituent on the aryl moiety (EDG *vs.* EWG). We have studied the dependence of the probe's fluorescence on the type of group at the *para*-phenyl position, for example, EWG *i.e.*, CF_3 in analogue **17**, *vs.* EDG, *i.e.*, OCH_3, in analogue **15**. Analogue **17**, 8-(4-trifluoromethyl-phenyl)-A, exhibited a longer emission wavelength as compared to the corresponding *p*-EDG substituted analogue **15**, (λ_{em} 439 *vs.* 394, 419 nm). Furthermore, the quantum yield of **17** was dramatically increased 160-fold as compared to that of **15** (ϕ 0.81 *vs.* 0.005).

Number of substituents on the aryl moiety. The dependence of fluorescence on the number of methoxy groups on the phenyl moiety was evaluated by comparing analogue **9**, 8-(4-methoxy-phenyl)-dA, to **10**, 8-(3,4,5-methoxy-phenyl)-dA. Addition of an EDG at the *meta* positions of analogue **10**, did not change the emission wavelength of analogue **9** (365, 385 nm, as compared to

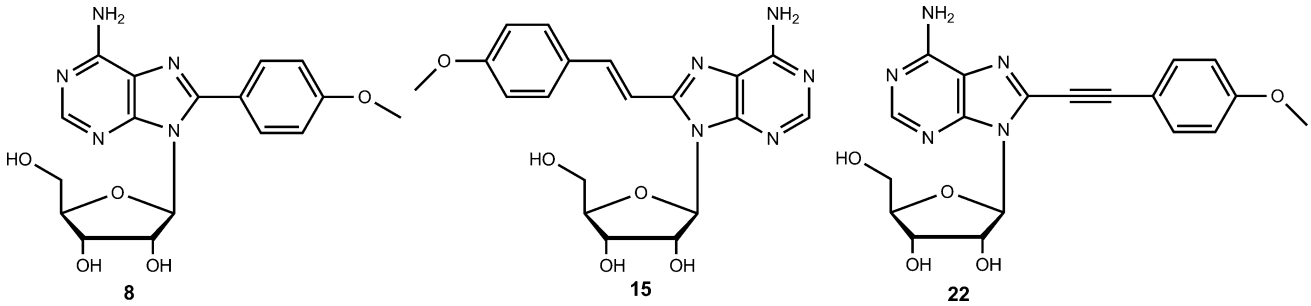

Fig. 4 Nucleoside analogues selected for conformational analysis.

362, 381 nm for analogue **9**). Furthermore, the quantum yield of **10** has decreased (0.46 *vs.* 0.113 in analogue **10**).

Aryl *vs.* heteroaryl substituent. The effect of the type of the aryl moiety on the fluorescence of adenosine was evaluated by comparing analogue **7** (aryl = Ph) to **12–14** (aryl = furyl or thiophenyl). We noticed that the nature of the aryl group directly coupled to the adenosine C8 position, whether phenyl or heteroaryl (furyl or thiophenyl) does not make a significant difference in maximum emission, *i.e.*, λ_{em} values of **7, 13** and **14** were 387, 381, 382 nm, ϕ values were 0.11, 0.46, 0.21, respectively. Unlike the latter compounds, analogue **12** (aryl = 5-methyl-2-thiophenyl), exhibited a relatively short emission wavelength (354 nm) and a low quantum yield (0.054).

Type of nucleobase. We also compared the properties of 8-(4-methoxy-phenyl)-A, **8**, 8-(2-(4-methoxyphenyl)-ethenyl)-A, **15**, and 8-((4-methoxyphenyl)-ethynyl)-A, **22**, to the corresponding G analogues **11, 20**, and **25**, respectively, to evaluate the contribution of the nucleobase to fluorescence. Analogues **8** and **11** exhibited the same emission wavelengths. Similar observations were made for analogues **15** and **20**. However, analogue **22** exhibited emission wavelength longer by ~40 nm than **25**.

In summary, analogues bearing an alkenyl linker at the purine C8 position (**15–21**), exhibited the longest emission wavelengths 408–439 nm, compared to the analogues in which the aryl/heteroaryl groups were linked directly to the nucleobase (~380 nm), analogues **7–14**, or *via* an alkynyl linker (~380 nm), analogues **22–25**. Extremely large quantum yields (~0.8) were found for analogues **17** and **21** bearing a *p*-EWG-Ph on an alkenyl linker. Substitutions of EDG at the phenyl *meta* position do not shift the emission wavelength of the probe. Conjugation of either aryl or heteroaryl to A or G resulted in similar emission wavelengths. Likewise, the purine nucleobase (A *vs.* G) does not affect the nucleoside probe fluorescence. High quantum yields were determined for analogues **9, 13**, and **14**, bearing aryl/heteroaryl groups directly linked to the nucleobase (ϕ 0.46, 0.46 and 0.21). Yet, substitution of an EWG instead of an EDG at the phenyl *para* position, as in analogue **17** *vs.* **15**, respectively, causes a dramatic 160-fold enhancement of the quantum yield (~0.8), and a 57 nm bathochromic shift of maximum emission.

Conformational analysis of analogues 8, 15, and 22

Extension of the natural fluorophore of purines by a large C8 substitution is expected to shift the nucleoside conformational equilibrium to favor the *syn* conformation, due to steric hindrance. When a nucleos(t)ide possessing a predominant *syn* conformation is incorporated into an oligonucleotide, which in turn undergoes hybridization to form a duplex, it might cause considerable destabilization of the B-DNA duplex structure and possibly enhance Z-DNA formation. To learn the possible consequences of incorporation of nucleoside analogues **7–25** in DNA duplexes, we studied by NMR the dependence of the *syn–anti* equilibrium and the ribose sugar puckering on the linkers of three representative analogues, **8, 15** and **22** (Fig. 4).

The representative nucleoside analogues **8, 15**, and **22**, bear at the purine C8 position a *p*-methoxyphenyl moiety linked directly or indirectly *via* an alkenyl or an alkynyl linker (Fig. 4). These analogues are ribonucleosides, but we assume that the 2′-deoxyribose analogues will exhibit similar characteristics.

Purine nucleosides in solution undergo rapid *syn*/*anti* interchange.[32] However, the ratio of *syn*/*anti* conformers is controlled by chemical modifications of the base. Specifically, 8-substituted purines may favor *syn* conformation due to steric hindrance between the 8-substituent and the ribose ring.[33,34]

The furanose ring in nucleosides does not possess a rigid structure in solution, but interconverts between South (*S*) and North (*N*) conformers.[35] In solution, both states are in equilibrium, however, in helical polynucleotides, the conformation is fixed in either *S* or *N* form.[36] In the common B-DNA structure the ribose conformation is *South*.[36]

The conformation around the glycosidic bond was qualitatively determined for analogues **8, 15**, and **22** by NOESY experiments, indicating typical H–H interactions between the ribose ring protons and the 8-substituent or the nucleobase. Specifically, the ^{1}H–^{1}H-NOESY spectrum of analogue **22**, indicated clear cross peaks between H1′ and H_a, and between H1′ and H_b (Fig. 5). In addition, a clear cross peak was observed between H2 and H(5′-OH), indicating a predominant *syn* conformation around the glycosidic bond. ^{1}H–^{1}H-NOESY spectrum of analogue **15** indicated clear cross peaks between H1′/H2′ and H-vinyl, in addition to a cross peak between H5′ and H-Ar, indicating a predominant *anti* conformation around the glycosidic bond (Fig. 5). In the same way, the predominant conformation of analogue **8** was determined and found to be *syn* (Table 2).

The conformation of the D-ribose ring of nucleosides **8, 15**, and **22** was analyzed in terms of a dynamic equilibrium in solution between the two favored puckered conformations: *N* and *S* conformers.[37–39] We calculated *N* and *S* equilibrium populations from observed $J_{1'2'}$ and $J_{3'4'}$ couplings for compounds **8**, **15**, and **22**, as previously reported.[37] The observed vicinal couplings are

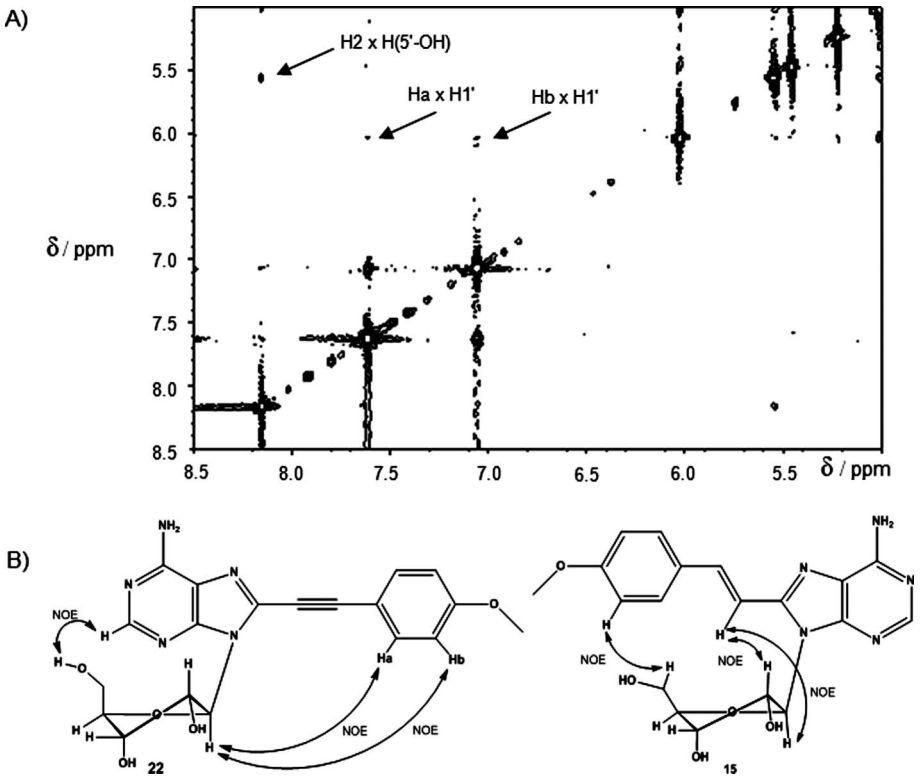

Fig. 5 Determination of the conformation of compounds **15** and **22**. A) ^{1}H,^{1}H-NOESY spectrum of compound **22**; B) NOE interactions in **15** and **22**.

Table 2 Conformational data of analogues **8, 15**, and **22** as determined by NMR

Analogue	Conformation around the glycosidic bond	Sugar puckering	
		X_S (%)	X_N (%)
8	*syn*	81	19
15	*anti*	76	24
22	*syn*	68	32

related to the relative proportion of conformers, given by eqn (1)–(3):

$$J_{1'2'} = 9.3(1 - X_N) + 9.3X_S \quad (1)$$

$$J_{2'3'} = 4.6X_N + 5.3(1 - X_N) \quad (2)$$

$$J_{3'4'} = 9.3X_N \quad (3)$$

Using the assigned *J*-coupling constants and the above equations, the mole fractions of conformers *S* and *N* for nucleotides **8, 15**, and **22** were calculated (Table 2). For all three analogues the predominant ribose puckering is *S*, ranging from 68 up to 81% of the conformers' population.

Discussion

We have designed and synthesized analogues **7–25** as novel fluorescent nucleoside probes based on a minimal extension of the non-fluorescent adenosine or guanosine chromophore. In these nucleoside analogues, the purine C8-position was conjugated either directly, or through an alkenyl or alkynyl linker, to an aryl/hetero aryl moiety. These extensions of the natural purine nucleobases significantly enhanced the spectral properties of the latter. For instance, the quantum yields of analogues **9** and **21** are 1770 and 3100-fold higher than adenosine and guanosine, respectively, and emission is red shifted by 60 and 156 nm, respectively.

Moreover, some of our new analogues exhibited better spectral characteristics than currently used purine fluorescent probes. For example, 2-amino adenosine, **5**,[19] and 8-vinyladenosine, **1**,[17] have high quantum yields (ϕ 0.65 and 0.66, respectively) and therefore, are useful probes for monitoring the structure and dynamics of DNA and for detecting base stacking in a duplex. These studies are based on the significant change in quantum yield of the probe upon incorporation into single-strand and double-strand oligonucleotide.[17,19,40,41] However, both 2-amino adenosine and 8-vinyladenosine emit at relatively short wavelengths, ~370 and 360 nm, respectively, while some of our purine derivatives emit at longer wavelengths with higher quantum yield (*e.g.* compound **17** – λ_{em} 439 nm; ϕ 0.81).

The enhanced fluorescence of some of our analogues may be attributed to the fact that they undergo an intramolecular charge transfer (ICT) from the donor to the acceptor moiety in the molecule.[42,43] In analogue **9**, the adenine moiety is the acceptor and the aryl moiety is the donor, while in analogue **17** the adenine is the donor and the aryl group is the acceptor.

Internal charge transfer process from the donor to the acceptor *via* the linker results in a large dipole moment in the excited state compared to that of the ground state, therefore the excited state is

more stabilized by the polar solvents and the excited-state energy is lowered, resulting in longer emission wavelengths.[44–46]

All directly conjugated adenosine and guanosine analogues, **7–14** (except analogue **12**), exhibited high quantum yields (>0.1), especially analogues **9** and **13** with a quantum yield of 0.46. However, as shown for analogue **8**, directly conjugated adenosine and guanosine analogues adopt preferentially the *syn* conformation due to steric hindrance between the aryl/heteroaromatic moiety at the C-8 position and the ribose ring. Adenosine and guanosine analogues **7–14** may not be attractive as fluorescent probes for incorporation in oligonucleotides, because their *syn* conformation might enhance the formation of the thermodynamically less stable Z-DNA duplex.

The alkenyl conjugated nucleoside analogues **15–21** displayed longer excitation and emission wavelengths as compared to directly conjugated analogues **7–14** (λ_{em} 408–459 nm) as anticipated according to the ICT theory. In addition to long λ_{em} values, a major advantage of analogues **15–21** is their preferred *anti* conformation. The phenyl moiety is shifted away from the ribose ring by the (*E*)-configured vinyl linker, thus minimizing steric hindrance and enabling the nucleoside standard *anti* conformation. Furthermore, a population of *ca.* 80% *Southern* sugar puckering indicates that upon incorporation into an oligonucleotide, followed by hybridization with target nucleic acid, analogues **15–21** are expected to contribute to the formation of stable B-DNA duplex. Analogues **15, 16**, and **20**, where the purine moiety is an acceptor, exhibited the lowest quantum yields of all analogues (≤0.018), a fact that may reduce their usefulness as fluorescent probes. However, analogues **17** and **21**, where the purine moiety is a donor, have the highest quantum yields (ϕ 0.81 and 0.8, respectively) and the longest emission wavelengths (λ_{em} 439 nm and 459 nm, respectively). Namely, purine nucleosides play either the acceptor or the donor role in push–pull systems **15–21**. Yet, dramatically enhanced fluorescence is obtained when the purine moiety plays the donor role in those push–pull molecules.[47]

For the alkynyl conjugated analogues **22–25**, we also anticipated long λ_{em} values, as for the alkenyl conjugated nucleosides; however, they exhibited relatively short emission wavelengths (≤385 nm). This phenomenon has been reported for *p*-amino styryl-naphthalene derivatives with different linkers between the aryl moieties,[48] and was explained by the delocalization of charge along the π system which includes more resonance structures for the alkenyl containing compound than for the alkynyl containing compound (Scheme 1). In addition, as shown for analogue **22**, alkynyl conjugated compounds adopt the undesired *syn* conformation due to steric hindrance between the alkynylaryl moiety and the ribose ring. Therefore, analogues **22–25** may not be suitable for incorporation in oligonucleotides to make fluorescent probes.

The changes in the λ_{em} between A and G analogues bearing the same donor moieties were not significant, *e.g.* the adenine analogue **8** and the guanine analogue **11** exhibited the same emission wavelength (~360 and 380 nm). Therefore, we conclude that the nucleobase does not have a significant effect on fluorescence.

To our surprise, there was a difference in the fluorescent properties of the ribose analogues compared to their corresponding 2′-deoxyribose analogues, yet no clear dependence of fluorescence on the presence of 2′-OH could be found. For instance, the 2′-deoxyribose analogue **9** had higher quantum yield (~4-fold) than the ribose analogue **8**, but the same emission wavelength. However, the 2′-deoxyribose analogue **16** had lower quantum yield (2-fold) than the ribose analogue **15**, and the emission wavelength was slightly shorter (408 *vs.* 419 nm).

Probes **7–25**, upon incorporation in oligonucleotides, were designed to be used in cells, but, fluorescence microscopy analysis requires probes with long absorption and emission wavelengths, due to auto-fluorescence of cells.[49] Therefore, out of analogues **7–25**, the alkenyl conjugated nucleoside analogues, **15–21**, are our most promising candidates as fluorescent probes, in particular, analogues **17** and **21** with the longest emission wavelength and the extremely high quantum yield.

The promising nucleoside probes will be eventually incorporated in oligonucleotides to be used for identification of target nucleic acids by hybridization assays. In those hybridization assays a B-DNA, rather than Z-DNA, structure is desired for the duplexes between probes and target nucleic acids, due its higher thermodynamic stability. Yet, the DNA conformation depends on various factors including chemical modifications of the bases,[50] which may affect *syn*/*anti* [51,52] or *S*/*N* conformers.

To ensure that our planned duplexes will adopt B-DNA structure, the conformation around the glycosidic bond and sugar puckering were determined for selected nucleoside probes. As was shown for analogue **15**, the alkenyl conjugated nucleoside analogues adopt preferentially the *anti* and *S* conformation, which may induce the formation of the favored B-DNA.

The potential of compounds **17** and **21** (and the corresponding 2′-deoxy-analogues) for the detection and quantification of genetic material upon incorporation in oligonucleotide probes will be reported in due course.

Experimental section

General

^{1}H-NMR and ^{13}C-NMR spectra were obtained on Bruker AC-200 and DPX-300 and DMX-600 spectrometers. For conformational analysis ^{1}H-NMR and NOESY spectra were obtained on Bruker DMX-600 with DMSO-d_6 as solvent. Chemical shifts are expressed in ppm downfield from Me_4Si (TMS) used as internal standard. The values are given in δ scale. All moisture sensitive reactions were carried out in flame-dried reactions flasks with rubber septa, and the reagents were introduced with a syringe. Progress of the reaction was monitored by TLC on precoated Merck silica gel plates (60F-254). Visualization was accomplished by UV light. Flash chromatography was carried out on silica gel (Davisil Art. 1000101501). Medium pressure chromatography was carried out using automated flash purification system (Biotage SP1 separation system, Uppsala, Sweden). The purity of the analogues was evaluated on HPLC (Merck-Hitachi) system, using an analytical reverse-phase column (Gemini 5u, C-18, 110A, 150 × 4.60 mm, 5 micron, Phenomenex, Torrance, CA, USA), in two solvent systems as described below. The purity of the nucleosides was generally ≥95%. New compounds were analyzed under ESI (electron spray ionization) conditions on a Q-TOF micro-instrument (Waters, UK). High resolution mass spectra were recorded on an AutoSpec Premier (Waters, UK) spectrometer by chemical ionization. Absorption spectra were measured on a UV instrument (UV-2401PC UV–VIS recording spectrophotometer, Shimadzu, Kyoto, Japan). Emission spectra were measured using

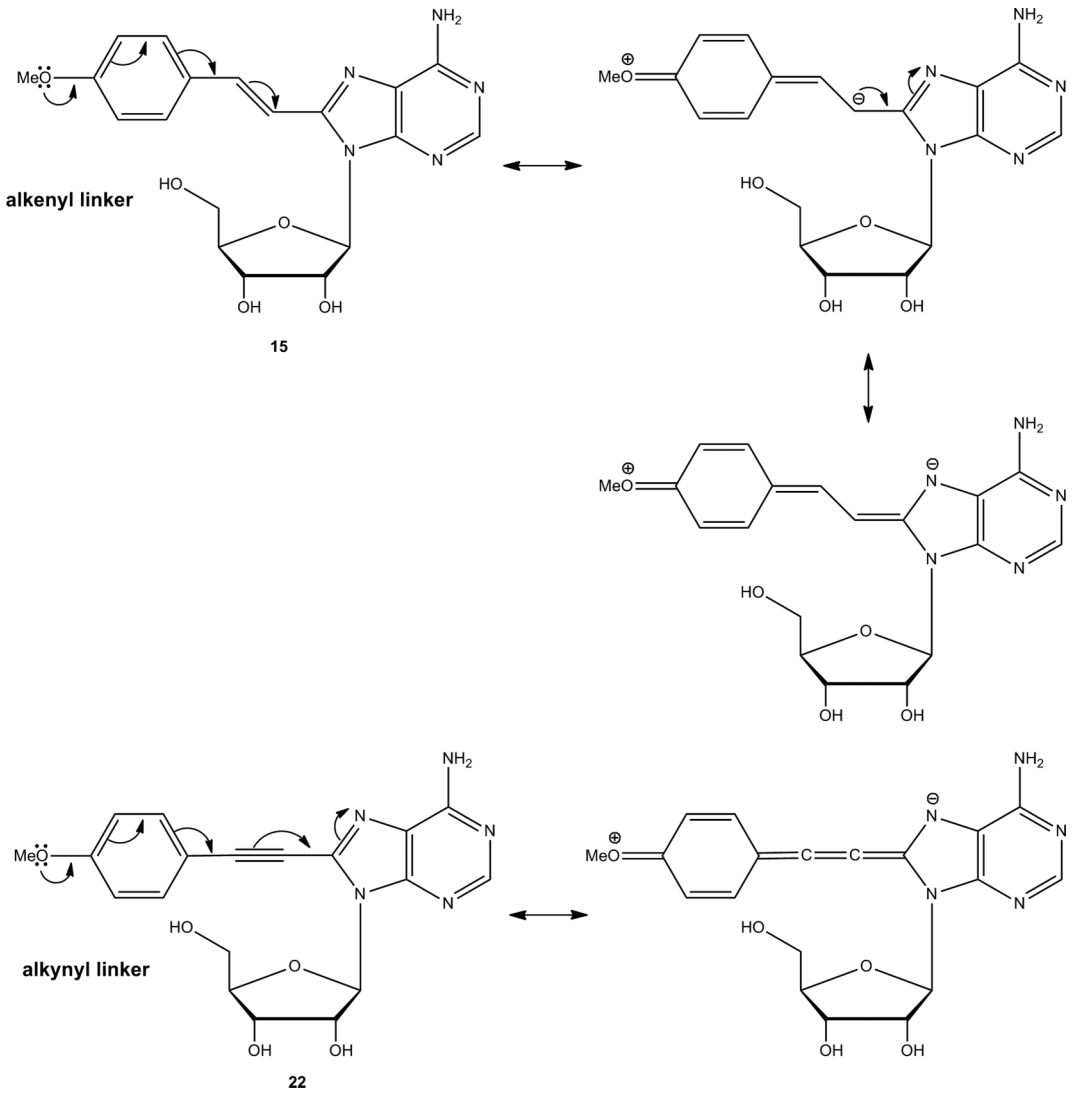

Scheme 1 Resonance structures of analogues **15** and **22**.

Aminco-Bowman series 2 (AB2) Luminescence Spectrometer (Thermo electron corporation, Markham, Ontario, Canada). As a standard we used tryptophan in H_2O (λ_{ex} 286 nm, λ_{em} 355 nm, ϕ 0.13), or quinine sulfate in H_2O (λ_{ex} 350 nm, λ_{em} 446 nm, ϕ 0.54).[27] Analogues **7**,[53] **8**,[53] **9**,[54]**11**,[22] **14**,[55] **22**,[56] and **25**[24] were synthesized according to the literature.

General procedure for the preparation of analogues 7–21

Water–acetonitrile (2 : 1, 3 mL) solvent mixture was added through a septum to an argon-purged round bottom flask containing 8-bromoadenosine (0.29 mmol, 1 eq) or 8-bromoguanosine (0.27 mmol, 1 eq), $Pd(OAc)_2$ (0.014 mmol, 0.05 eq), sodium carbonate (0.86 mmol, 3 eq), TPPTS (0.072 mmol, 0.25 eq), and the appropriate boronic acid derivative (0.36 mmol, 1.25 eq). The mixture was stirred at 90 °C under argon atmosphere for ~2 h. The reaction was cooled to room temperature and few drops of 37% HCl were added (up to pH~7). The product was purified on a silica gel column using $CHCl_3$: MeOH, 8 : 2, as the eluent.

General procedure for the preparation of analogues 22–25

To a solution of 8-bromoadenosine (0.43 mmol, 1 eq) or 8-bromoguanosine (0.41 mmol, 1 eq) in dry DMF (12.7 mL), and Et_3N (1.95 mL) under an atmosphere of Ar were added tetrakis(triphenylphosphine)palladium (0.043 mmol, 0.1 eq) and CuI (0.003 mmol). The appropriate terminal alkyne (1.29 mmol, 3 eq) was added and the reaction mixture was stirred at room temperature for overnight. The solvent was removed *in vacuo* and the residue was purified on a silica gel column using $CHCl_3$: MeOH, 8 : 2, as the eluent.

5-(6-Amino-8-(3,4,5-trimethoxyphenyl)-9*H*-purin-9-yl)-2-(hydroxymethyl)tetrahydrofuran-3-ol (10)

Product **10** was obtained as an orange solid (110 mg, 87%), starting from 8-Br-2′-deoxy-adenosine (100 mg, 0.303 mmol) and 3,4,5-trimethoxyphenylboronic acid. Mp 118–119 °C; ^{1}H-NMR (300 MHz, DMSO-d_6): δ 8.14 (s, 1H, 2-H), 7.43 (s, 2H, NH_2), 7.00 (s, 2H, Ph-H), 6.20 (dd, J = 8.3 and 5.5 Hz, 1H, 1′-H), 5.59 (dd, J = 8.5 and 3.9 Hz, 1H, OH), 5.26 (d, J = 4.6 Hz,1H, OH),

4.45 (m, 1H, 3′-H), 3.86 (m, 1H, 4′-H), 3.84 (s, 6H, m-OCH_3), 3.76 (s, 3H, p-OCH_3), 3.68 (m, 1H, 5′-H), 3.52 (m, 1H, 5″-H), 3.20 (m, 1H, 2′-H), 2.20 (m, 1H, 2″-H) ppm; ^{13}C-NMR (75 MHz, DMSO-d_6): δ 156.1, 152.9, 151.9, 150.4, 149.9, 138.9, 124.8, 119.0, 107.0, 88.3, 85.8, 71.5, 62.4, 60.2, 56.1, 37.4 ppm. Purity data obtained on an analytical column: t_R 6.4 min, using solvent system I (85 : 15 to 50 : 50 H_2O : CH_3CN over 10 min, 1 mL min^{-1}) 95% purity; t_R 5.46 min, solvent system II (60 : 40 to 20 : 80 H_2O : MeOH over 10 min, 1 mL min^{-1}) 97% purity. UV–vis (CH_3OH) λ_{max} 292 nm. MS ES+ *m/z*: 418 (MH^+); HR MALDI calcd for $C_{19}H_{24}N_5O_6$: 418.2376, found 418.1721.

2-(6-Amino-8-(5-methylthiophen-2-yl)-9*H*-purin-9-yl)-5-(hydroxymethyl)tetrahydrofuran-3,4-diol (12)

Product **12** was obtained as a white solid (25 mg, 24%), starting from 8-Br-adenosine (100 mg, 0.29 mmol) and 5-methyl-2-thiopheneboronic acid. Mp 210–211 °C (dec); ^{1}H-NMR (300 MHz, DMSO-d_6): δ 8.12 (s, 1H, 2-H), 7.48 (s, 2H, NH_2), 7.45 (d, *J* = 3.4 Hz, 1H, CH), 6.99 (d, *J* = 3.4 Hz, 1H, CH), 5.99 (d, *J* = 7.1 Hz, 1H, 1′-H), 5.79 (dd, *J* = 8.7 and 3.2 Hz, 1H, OH), 5.50 (d, *J* = 6.3 Hz, 1H, OH), 5.19 (m, 1H, OH), 5.18 (m, 1H, 2′-H), 4.20 (m, 1H, 3′-H), 3.97 (m, 1H, 4′-H), 3.68 (ddd, *J* = 12, 6.7, and 3 Hz, 1H, 5′-H), 3.56 (ddd, *J* = 12, 9.6, and 3.70 Hz, 1H, 5″-H), 2.54 (s, 3H, CH_3) ppm; ^{13}C-NMR (75 MHz, DMSO-d_6): δ 155.9, 152.0, 149.8, 145.1, 143.7, 130.1, 128.1, 126.6, 119.1, 89.1, 86.7, 71.3, 71.0, 62.2, 14.9 ppm. Purity data obtained on an analytical column: t_R 6.67 min, using solvent system I (85 : 15 to 50 : 50 H_2O : CH_3CN over 10 min, 1 mL min^{-1}) 96% purity; t_R 6.14 min, solvent system II (60 : 40 to 20 : 80 H_2O : MeOH over 10 min, 1 mL min^{-1}) 95% purity. UV–vis (CH_3OH) λ_{max} 309 nm. MS ES+ *m/z*: 364 (MH^+); HR MALDI calcd for $C_{15}H_{17}N_5NaO_4S$: 386.2363, found 386.0893.

5-(6-Amino-8-(furan-2-yl)-9*H*-purin-9-yl)-2-(hydroxymethyl)tetrahydrofuran-3-ol (13)

Product **13** was obtained as a white solid (85 mg, 89%), starting from 8-Br-2′-deoxy-adenosine (100 mg, 0.303 mmol) and 2-furanboronic acid. Mp 186 °C (dec); ^{1}H-NMR (300 MHz, DMSO-d_6): δ 8.13 (s, 1H, 2-H), 8.01 (dd, *J* = 1.8 and 0.8 Hz, 1H,CH), 7.49 (s, 2H, NH_2), 7.12 (dd, *J* = 3 and 0.8 Hz, 1H, CH), 6.78 (dd, *J* = 3 and 1.8 Hz, 1H, CH), 6.54 (dd, *J* = 8 and 6.3 Hz, 1H, 1′-H), 5.50 (dd, *J* = 8.2 and 4 Hz, 1H, OH), 5.30 (d, *J* = 3.2 Hz, 1H, OH), 4.50 (m, 1H, 3′-H), 3.90 (m, 1H, 4′-H), 3.67 (ddd, *J* = 11.8, 7.8, and 4 Hz, 1H, 5′-H), 3.52 (ddd, *J* = 11.8, 7.8, and 4.5 Hz, 1H, 5″-H), 3.29 (m, 1H, 2′-H), 2.19 (ddd, *J* = 13.2, 6.3, and 2.6 Hz, 1H, 2″-H) ppm; ^{13}C-NMR (150 MHz, DMSO-d_6): δ 156.1, 152.2, 149.6, 145.4, 143.5, 141.0, 119.4, 113.6, 112.1, 88.3, 85.5, 71.3, 62.2, 37.5 ppm. Purity data obtained on an analytical column: t_R 4.6 min, using solvent system I (75 : 25 to 50 : 50 H_2O : CH_3CN over 10 min, 1 mL min^{-1}) 95% purity; t_R 5.93 min, solvent system II (60 : 40 to 20 : 80 H_2O : MeOH over 10 min, 1 mL min^{-1}) 95% purity. UV–vis (CH_3OH) λ_{max} 306 nm. MS ES+ *m/z*: 318 (MH^+); HR MALDI calcd for $C_{14}H_{15}N_5O_4$: 318.1714, found 318.1197.

2-(6-Amino-8-(4-methoxystyryl)-9*H*-purin-9-yl)-5-hydroxymethyl)tetrahydrofuran-3,4-diol (15)

Product **15** was obtained as a yellow solid (47 mg, 42%), starting from 8-Br-adenosine (100 mg, 0.29 mmol) and *trans*-2-(4-methoxyphenyl)vinylboronic acid. Mp 228–229 °C (dec); ^{1}H NMR (600 MHz, DMSO-d_6): δ 8.26 (s, 1H, H-2), 7.75 (d, *J* = 14 Hz, 1H, CH), 7.73 (d, *J* = 8.7 Hz, 2H, Ph-H), 7.47 (d, *J* = 14 Hz, 1H, CH), 7.00 (d, *J* = 8.7 Hz, 2H, Ph-H), 6.14 (d, *J* = 6.9 Hz, 1H, H-1′), 4.68 (t, *J* = 6.9 Hz, 1H, H-2′), 4.22 (dd, *J* = 4.9 and 1.9 Hz, 1H, H-3′), 4.02 (m, 1H, H-4′), 3.81 (s, 3H, CH_3), 3.73 (m, 1H, H-5′), 3.64 (m, 1H, H-5″) ppm; ^{13}C-NMR (150 MHz, DMSO-d_6): δ 160.3, 158.8, 149.9, 149.7, 137.0, 129.4, 128.1, 127.4, 118.8, 114.4, 112.0, 87.5, 86.4, 72.7, 70.1, 61.5, 55.3 ppm. Purity data obtained on an analytical column: t_R 4.59 min, using solvent system I (75 : 25 to 50 : 50 H_2O : CH_3CN over 10 min, 1 mL min^{-1}) 95% purity; t_R 6.5 min, solvent system II (60 : 40 to 20 : 80 H_2O : MeOH over 10 min, 1 mL min^{-1}) 98% purity. UV–vis (CH_3OH) λ_{max} 345 nm. MS ES+ *m/z*: 400 (MH^+); HR MALDI calcd for $C_{19}H_{22}N_5O_5$: 400.1615, found 400.1621.

5-(6-Amino-8-((*E*)-4-methoxystyryl)-9*H*-purin-9-yl)-2-(hydroxymethyl)tetrahydrofuran-3-ol (16)

Product **16** was obtained as a yellow solid (96 mg, 83%), starting from 8-Br-2′-deoxy-adenosine (100 mg, 0.303 mmol) and *trans*-2-(4-methoxyphenyl)vinylboronic acid. Mp 230–231 °C (dec); ^{1}H-NMR (300 MHz, DMSO-d_6): δ 8.09 (s, 1H, 2-H), 7.71 (d, *J* = 8.6 Hz, 2H, Ph-H), 7.68 (d, *J* = 15.7 Hz, 2H, CH), 7.45 (d, *J* = 15.7 Hz, 2H, CH), 7.28 (s, 2H, NH_2), 6.98 (d, *J* = 8.6 Hz, 2H, Ph-H), 6.59 (dd, *J* = 5.7 and 1.4 Hz, 1H, 1′-H), 5.49 (dd, *J* = 6.9 and 4.1 Hz, 1H, OH), 5.31 (d, *J* = 4.1 Hz, 1H, OH), 4.51 (m, 1H, 3′-H), 3.89 (m, 1H, 4′-H), 3.80 (s, 3H, O-CH_3), 3.71 (m, 1H, 5′-H), 3.59 (m, 1H, 5″-H), 2.93 (m, 1H, 2′-H), 2.19 (m, 1H, 2″-H) ppm; ^{13}C-NMR (75 MHz, DMSO-d_6): δ 160.1, 155.5, 151.7, 149.9, 148.3, 135.9, 129.1, 128.4, 119.1, 114.3, 112.6, 87.8, 83.4, 70.7, 61.7, 55.3 ppm. Purity data obtained on an analytical column: t_R 8.35 min, using solvent system I (85 : 15 to 50 : 50 H_2O : CH_3CN over 10 min, 1 mL min^{-1}) 99% purity; t_R 5.93 min, solvent system II (50 : 50 to 20 : 80 H_2O : MeOH over 10 min, 1 mL min^{-1}) 95% purity. UV–vis (CH_3OH) λ_{max} 340 nm. MS ES+ *m/z*: 384 (MH^+); HR MALDI calcd for $C_{19}H_{21}N_5O_4$: 384.2238, found 384.1666.

2-(6-Amino-8-((*E*)-4-(trifluoromethyl)styryl)-9*H*-purin-9-yl)-5-(hydroxymethyl)tetrahydrofuran-3,4-diol (17)

Product **17** was obtained as a white solid (70 mg, 55%), starting from 8-Br-adenosine (100 mg, 0.29 mmol) and *trans*-2-[4-(trifluoromethyl)phenyl]vinylboronic acid. Mp 212–213 °C (dec); ^{1}H-NMR (200 MHz, DMSO-d_6): δ 8.12 (s, 1H, 2-H), 7.98 (d, *J* = 7.6 Hz, 2H, Ph-H), 7.78 (s, 2H, CH), 7.76 (d, *J* = 7.6 Hz, 2H, Ph-H), 7.46 (s, 2H, NH_2), 6.16 (d, *J* = 7 Hz, 1H, 1′-H), 5.82 (dd, *J* = 7.5 and 3.5 Hz, 1H, OH), 5.37 (d, *J* = 6.5 Hz, 1H, OH), 5.26 (d, *J* = 4.5 Hz, 1H, OH), 4.71 (m, 1H, 2′-H), 4.20 (m, 1H, 3′-H), 4.03 (m, 1H, 4′-H), 3.71- 3.65 (m, 2H, 5′-H and 5″-H) ppm; ^{13}C-NMR (50 MHz, DMSO-d_6): δ 155.8, 152.2, 150.1, 147.5, 139.7, 134.4, 128.4, 128.1, 125.6, 117.8, 87.5, 86.5, 72.8, 70.4, 61.8 ppm. Purity data obtained on an analytical column: t_R 9.67 min, using solvent system I (75 : 25 to 50 : 50 H_2O : CH_3CN over 10 min, 1 mL min^{-1}) 99% purity; t_R 6.57 min, solvent system II (90 : 10 to 70 : 30 MeOH : CH_3CN over 10 min, 1 mL min^{-1}) 98% purity. UV–vis (CH_3OH) λ_{max} 340 nm. MS ES+ *m/z*: 438 (MH^+); HR MALDI calcd for $C_{19}H_{18}F_3N_5O_4$: 437.3762, found 438.1380.

5-(6-Amino-8-(4-(trifluoromethyl)styryl)-9*H*-purin-9-yl)-2-(hydroxymethyl)tetrahydrofuran-3-ol (18)

Product **18** was obtained as a yellow solid (82 mg, 65%), starting from 8-Br-2′-deoxy-adenosine (100 mg, 0.303 mmol) and *trans*-2-[4-(trifluoromethyl)phenyl] vinylboronic acid. Mp 219–220 °C (dec); ^{1}H-NMR (200 MHz, DMSO-d_6): δ 8.12 (s, 1H, 2-H), 7.99 (d, J = 7.78 Hz, 2H, Ph-H), 7.86 (d, J = 12.46 Hz, 1H, CH), 7.77 (d, J = 12.46 Hz, 1H, CH), 7.76 (d, J = 7.78 Hz, 2H, Ph-H), 7.41 (s, 2H, NH_2), 6.64 (t, J = 7.78 Hz, 1H, 1′-H), 5.46 (t, J = 4.67 Hz, 1H, OH), 5.34 (d, J = 4.67 Hz, 1H, OH), 4.52 (m, 1H, 3′-H), 3.92 (m, 1H, 4′-H), 3.70–3.60 (m, 2H, 5′-H and 5″-H), 2.91 (m, 1H, 2′-H), 2.22 (m, 1H, 2″-H) ppm; ^{13}C-NMR (150 MHz, DMSO-d_6): δ 155.7, 152.8, 149.9, 147.3, 139.7, 134.2, 128.5, 127.6, 125.7, 120.3, 119.2, 118.1, 87.9, 83.5, 70.1, 61.6, 39.2 ppm. Purity data obtained on an analytical column: t_R 6.84 min, using solvent system I (65 : 35 to 50 : 50 H_2O : CH_3CN over 10 min, 1 mL min^{-1}) 95% purity; t_R 7.47 min, solvent system II (90 : 10 to 70 : 30 MeOH : CH_3CN over 10 min, 1 mL min^{-1}) 98% purity. UV–vis (CH_3OH) λ_{max} 338 nm. MS ES+ m/z: 423 (MH^+); HR MALDI calcd for $C_{19}H_{19}F_3N_5O_3$: 422.3836, found 422.1435.

2-(6-Amino-8-(4-fluorostyryl)-9*H*-purin-9-yl)-5-(hydroxymethyl)tetrahydrofuran-3,4-diol (19)

Product **19** was obtained as a yellow solid (45 mg, 40%), starting from 8-Br-adenosine (100 mg, 0.29 mmol) and *trans*-2-(4-fluorophenyl)vinylboronic acid. Mp 215–216 °C (dec); ^{1}H-NMR (200 MHz, DMSO-d_6): δ 8.10 (s, 1H, 2-H), 7.82 (m, 2H, Ph-H), 7.74 (d, J = 15.88 Hz, 1H, CH), 7.53 (d, J = 15.88 Hz, 1H, CH), 7.40 (s, 2H, NH_2), 7.26 (m, 2H, Ph-H), 6.12 (d, J = 7.4 Hz, 1H, 1′-H), 5.82 (t, J = 3.7 Hz, 1H, OH), 5.35 (m,1H, OH), 5.27 (m, 1H, OH), 4.7 (m, 1H, 2′-H), 4.20 (m, 1H, 3′-H), 4.01 (m, 1H, 4′-H), 3.70–3.62 (m, 2H, 5′-H and 5″-H) ppm; ^{13}C-NMR (50 MHz, DMSO-d_6): δ 155.7, 151.9, 150.0, 148.1, 135.1, 132.4, 129.8, 129.6, 116.1, 115.6, 114.8, 87.6, 86.5, 72.7, 70.4, 61.8 ppm; ^{19}F-NMR (188 MHz, DMSO-d_6): δ –112.4 ppm. Purity data obtained on an analytical column: t_R 9.23 min, using solvent system I (85 : 15 to 50 : 50 H_2O : CH_3CN over 10 min, 1 mL min^{-1}) 98% purity; t_R 3.47 min, solvent system II (90 : 10 to 70 : 30 MeOH : CH_3CN over 10 min, 1 mL min^{-1}) 95% purity. UV–vis (CH_3OH) λ_{max} 333 nm. MS ES+ m/z: 388 (MH^+); HR MALDI calcd for $C_{18}H_{19}FN_5O_4$: 388.3771, found 388.1416.

2-Amino-9-(3,4-dihydroxy-5-(hydroxymethyl)tetrahydrofuran-2-yl)-8-(4-methoxystyryl)-1*H*-purin-6(9*H*)-one (20)

Product **20** was obtained as a yellow solid (10.8 mg, 10%), starting from 8-Br-guanosine (100 mg, 0.27 mmol) and *trans*-2-(4-methoxyphenyl)vinylboronic acid. Mp 205–206 °C (dec); ^{1}H NMR (600 MHz, DMSO-d_6): δ 7.64 (d, J = 8.2 Hz, 2H, Ph-H), 7.49 (d, J = 15.6 Hz, 1H, CH), 7.28 (d, J = 15.6 Hz, 1H, CH), 6.94 (d, J = 8.2 Hz, 2H, Ph-H), 6.47 (s, 2H, NH_2), 5.92 (d, J = 6.8 Hz, 1H, H-1′), 5.31 (m, 2H, OH), 5.07 (m, 1H, OH), 4.50 (m, 1H, H-2′), 4.16 (m, 1H, H-3′), 3.90 (m, 1H, H-4′), 3.79 (s, 3H, CH_3), 3.72 (m, 1H, H-5′), 3.65 (m, 1H, H-5″) ppm. Purity data obtained on an analytical column: t_R 5.57 min, using solvent system I (85 : 15 to 50 : 50 H_2O : CH_3CN over 10 min, 1 mL min^{-1}) 99% purity; t_R 6.96 min, solvent system II (70 : 30 to 30 : 70 H_2O : MeOH over 10 min, 1 mL min^{-1}) 99% purity. UV–vis (CH_3OH) λ_{max} 350 nm. MS ES+ m/z: 438 (MNa^+); HR MALDI calcd for $C_{19}H_{21}N_5NaO_6$: 438.1384, found 438.1371.

2-Amino-9-(3,4-dihydroxy-5-(hydroxymethyl)tetrahydrofuran-2-yl)-8-(4-(trifluoromethyl)styryl)-1*H*-purin-6(9*H*)-one (21)

Product **21** was obtained as a yellow–green solid (89 mg, 73%), starting from 8-Br-guanosine (100 mg, 0.27 mmol) and *trans*-2-[4-(trifluoromethyl)phenyl]vinylboronic acid. Mp 188–190 °C (dec); ^{1}H NMR (300 MHz, DMSO-d_6): 7.92 (d, J = 8.44 Hz, 2H, Ph-H), 7.70 (d, J = 8.44 Hz, 2H, Ph-H), 7.69 (d, J = 19 Hz, 1H, CH), 7.64 (d, J = 19 Hz, 1H, CH), 6.58 (s, 2H, NH_2), 5.96 (d, J = 7.39 Hz, 1H, H-1′), 5.38 (t, J = 5.23 Hz, 1H, OH), 5.34 (d, J = 5.23 Hz, 1H, OH), 5.10 (d, J = 3.49 Hz, 1H, OH), 4.45 (m, 1H, H-2′), 4.14 (m, 1H, H-3′), 3.92 (m, 1H, H-4′), 3.70 (m, 2H, H-5′ and H-5″) ppm; ^{13}C-NMR (150 MHz, DMSO-d_6): δ 156.3, 153.8, 152.3, 143.8, 140.3, 131.6, 131.1, 127.7, 125.6, 125.5, 123.4, 118.7, 116.8, 86.4, 85.6, 72.9, 69.8, 61.2 ppm. Purity data obtained on an analytical column: t_R 8.27 min, using solvent system I (75 : 25 to 50 : 50 H_2O : CH_3CN over 10 min, 1 mL min^{-1}) 99% purity; t_R 4.85 min, solvent system II (90 : 10 to 70 : 30 MeOH : CH_3CN over 10 min, 1 mL min^{-1}) 99% purity. UV–vis (CH_3OH) λ_{max} 357 nm. MS ES+ m/z: 476 (MNa^+); HR MALDI calcd for $C_{19}H_{18}F_3N_5NaO_5$: 476.1752, found 476.1152.

5-(6-Amino-8-((4-methoxyphenyl)ethynyl)-9*H*-purin-9-yl)-2-(hydroxymethyl)tetrahydrofuran-3-ol (23)

Product **23** was obtained as a brown solid (30 mg, 26%), starting from 8-Br-2′-deoxy-adenosine (100 mg, 0.303 mmol) and 4-ethynylanisole. Mp 167–168 °C (dec); ^{1}H-NMR (200 MHz, DMSO-d_6): δ 8.16 (s, 1H, 2-H), 7.63 (d, J = 8.3 Hz, 2H, Ph-H), 7.59 (s, 2H, NH_2), 7.06 (d, J = 8.3 Hz, 2H, Ph-H), 6.52 (dd, J = 7.1 and 6 Hz, 1H, 1′-H), 5.36 (d, J = 4.4 Hz, 1H, OH), 5.34 (dd, J = 7.4 and 4.4 Hz, 1H, OH), 4.50 (m, 1H, 3′-H), 3.92 (m, 1H, 4′-H), 3.83 (s, 3H, O-CH_3), 3.65 (m, 1H, 5′-H), 3.51 (m, 1H, 5″-H), 3.12 (m, 1H, 2′-H), 2.26 (m, 1H, 2″-H) ppm; ^{13}C-NMR (50 MHz, DMSO-d_6): δ 160.8, 155.9, 153.2, 148.5, 133.7, 133.3, 114.8, 111.7, 94.9, 88.3, 85.0, 77.6, 77.4, 71.3, 62.2, 55.5, 37.8 ppm. Purity data obtained on an analytical column: t_R 8.74 min, using solvent system I (85 : 15 to 50 : 50 H_2O : CH_3CN over 10 min, 1 mL min^{-1}) 98% purity; t_R 7.99 min, solvent system II (60 : 40 to 20 : 80 H_2O : MeOH over 10 min, 1 mL min^{-1}) 99% purity. UV–vis (CH_3OH) λ_{max} 323 nm. MS ES+ m/z: 381 (MH^+); HR MALDI calcd for $C_{19}H_{19}N_5O_4$: 382.2080, found 382.1510.

2-(6-Amino-8-((3,5-dimethoxyphenyl)ethynyl)-9*H*-purin-9-yl)-5-(hydroxymethyl)tetrahydrofuran-3,4-diol (24)

Product **24** was obtained as a pale yellow solid (117 mg, 95%), starting from 8-Br-adenosine (100 mg, 0.29 mmol) and 1-ethynyl-3,5-dimethoxybenzene. Mp 208 °C (dec); ^{1}H-NMR (300 MHz, DMSO-d_6): δ 8.18 (s, 1H, 2-H), 7.67 (s, 2H, NH_2), 6.82 (d, J = 2.3 Hz, 2H, Ph-H), 6.70 (t, J = 2.3 Hz, 1H, Ph-H), 6.04 (d, J = 6.6 Hz, 1H, 1′-H), 5.53 (dd, J = 8.6 and 3.9 Hz, 1H, OH), 5.48 (d, J = 6.5 Hz, 1H, OH), 5.25 (d, J = 4.7 Hz, 1H, OH), 5.00 (m, 1H, 2′-H), 4.20 (m, 1H, 3′-H), 4.00 (m, 1H, 4′-H), 3.81 (s, 6H, O-CH_3), 3.70 (m, 1H, 5′-H), 3.55 (m, 1H, 5″-H) ppm; ^{13}C-NMR (75 MHz, DMSO-d_6): δ 160.6, 156.2, 153.5, 148.6, 133.2, 121.3, 119.6, 109.7, 103.2, 94.3, 89.4, 86.7, 78.1, 71.8, 71.0, 62.2, 55.6,

45.8 ppm. Purity data obtained on an analytical column: t_R 6.61 min, using solvent system I (85 : 15 to 50 : 50 H_2O : CH_3CN over 10 min, 1 mL min^{-1}) 99% purity; t_R 6.32 min, solvent system II (50 : 50 to 20 : 80 H_2O : MeOH over 10 min, 1 mL min^{-1}) 99% purity. UV–vis (CH_3OH) λ_{max} 316 nm. MS ES+ *m/z*: 428 (MH^+); HR MALDI calcd for $C_{20}H_{21}N_5O_6$: 428.4228, found 428.1565.

Abbreviations

A	adenosine
G	guanosine
NOESY	Nuclear Overhauser Enhancement spectroscopy
TPPTS	tris(3-sulfonatophenyl) phosphine trisodium salt
EDG	electron donating group
EWG	electron withdrawing group
ICT	intramolecular charge transfer

References

1 D. P. Burma, *Quart. J. Surg. Sci.*, 1969, **5**, 114–126.
2 L. Gehrke, *Gene Anal. Tech.*, 1986, **3**, 45–52.
3 C Mougin, A. F. Guitteny, B. Fouque, G. Viennet, R. Teoule and B. Bloch, *J. Pathol.*, 1990, **160**, 187–194.
4 L. J. Kricka and P. Fortina, *Clin. Chem. (Washington, DC, U. S.)*, 2009, **55**, 670–683.
5 E. Nir, K. Kleinermanns, L. Grace and M. S. de Vries, *J. Phys. Chem. A*, 2001, **105**, 5106–5110.
6 P. R. Callis, *Annu. Rev. Phys. Chem.*, 1983, **34**, 329–357.
7 R. P. Haugland, *The Handbook - A guide to fluorescent probes and labeling technologies*, Invitrogen/Molecular Probes, Carlsbad, CA, 10th edn, 2005.
8 Z. G. Goldsmith and N. Dhanasekaran, *Int. J. Mol. Med.*, 2004, **13**, 483–495.
9 C. Fauth and M. R. Speicher, *Cytogenet. Cell Genet.*, 2001, **93**, 1–10.
10 B. Dummitt and Y.-H. Chang, *Assay Drug Dev. Technol.*, 2006, **4**, 343–349.
11 S. A. E. Marras, S. Tyagi and F. R. Kramer, *Clin. Chim. Acta*, 2006, **363**, 48–60.
12 G Yao, M. S. John and W. Tan, *Fluore. Sens. Biosens.*, 2006, 67–92.
13 P. R. Langer, A. A. Waldrop and D. C. Ward, *Proc. Natl. Acad. Sci. U. S. A.*, 1981, **78**, 6633–6637.
14 A. M. Femino, F. S. Fay, K. Fogarty and R. H. Singer, *Science*, 1998, **280**, 585–590.
15 D. W. Dodd and R. H. E. Hudson, *Mini-Rev. Org. Chem.*, 2009, **6**, 378–391.
16 M. Daniels and W. Hauswirth, *Science*, 1971, **171**, 675–677.
17 G. Kodali, K. A. Kistler, M. Narayanan, S. Matsika and R. J. Stanley, *J. Phys. Chem. A*, 2010, **114**, 256–267.
18 Nouha Ben Gaied, Nicole Glasser, Nick Ramalanjaona, Hervé Beltz, Philippe Wolff, Roland Marquet and A. B. a. Y. Mély, *Nucleic Acids Res.*, 2005, **33**, 1031–1039.
19 J. M. Jean and K. B. Hall, *Proc. Natl. Acad. Sci. U. S. A.*, 2001, **98**, 37–41.
20 E. Sharon, S. A. Levesque, M. N. Munkonda, J. Sevigny, D. Ecke, G. Reiser and B. Fischer, *ChemBioChem*, 2006, **7**, 1361–1374.
21 K. M. Sun, C. K. McLaughlin, D. R. Lantero and R. A. Manderville, *J. Am. Chem. Soc.*, 2007, **129**, 1894–1895.
22 P. Capek, R. Pohl and M. Hocek, *Org. Biomol. Chem.*, 2006, **4**, 2278–2284.
23 A. Collier and G. K. Wagner, *Synth. Commun.*, 2006, **36**, 3713–3721.
24 A. G. Firth, I. J. S. Fairlamb, K. Darley and C. G. Baumann, *Tetrahedron Lett.*, 2006, **47**, 3529–3533.
25 C. Lambertucci, S. Costanzi, S. Vittori, R. Volpini and G. Cristalli, *Nucleosides, Nucleotides Nucleic Acids*, 2001, **20**, 1153–1157.
26 E. C. Western, *thesis*, University of Alabama, 2005.
27 J. Yvon, A Guide to recording fluorescence quantum yields, http://www.jobinyvon.com.
28 S Fery-Forgues and D. Lavabre, *J. Chem. Educ.*, 1999, **76**, 1260–1264.
29 G. Favaro, A. Romani and R. S. Becker, *Photochem. Photobiol.*, 2001, **74**, 378–384.
30 R Borrelli and A. Peluso, *J. Chem. Phys.*, 2006, **125**, 194308.
31 T Petrenko, O. Krylova, F. Neese and M. Sokolowski, *New J. Phys.*, 2009, **11**, 015001.
32 P. A. Hart and J. P. Davis, *Jerusalem Symp. Quantum Chem. Biochem.*, 1973, **5**, 297–310.
33 S. S. Tavale and H. M. Sobell, *J. Mol. Biol.*, 1970, **48**, 109–123.
34 A. L. Millen, C. K. McLaughlin, K. M. Sun, R. A. Manderville and S. D. Wetmore, *J. Phys. Chem. A*, 2008, **112**, 3742–3753.
35 D. B. Davies, *Prog. Nucl. Magn. Reson. Spectrosc.*, 1978, **12**, 135–225.
36 W. Sanger, *Principles of nucleic acid structure*, Springer-Verlag, Berlin, 1984.
37 D. B. Davies and S. S. Danyluk, *Biochemistry*, 1974, **13**, 4417–4434.
38 C Altona and M. Sundaralingam, *J. Am. Chem. Soc.*, 1972, **94**, 8205–8212.
39 C Altona and M. Sundaralingam, *J. Am. Chem. Soc.*, 1973, **95**, 2333–2344.
40 T. M. Nordlund, S. Andersson, L. Nilsson, R. Rigler, A. Graeslund and L. W. McLaughlin, *Biochemistry*, 1989, **28**, 9095–9103.
41 M. J. Rist and J. P. Marino, *Curr. Org. Chem.*, 2002, **6**, 775–793.
42 R. S. Butler, P. Cohn, P. Tenzel, K. A. Abboud and R. K. Castellano, *J. Am. Chem. Soc.*, 2009, **131**, 623–633.
43 R. S. Butler, A. K. Myers, P. Bellarmine, K. A. Abboud and R. K. Castellano, *J. Mater. Chem.*, 2007, **17**, 1863–1865.
44 M. A. Haidekker and E. A. Theodorakis, *J. Biol. Eng.*, 2010, **4**, 11.
45 B. Kumar Paul, A. Samanta, S. Kar and N. Guchhait, *J. Lumin.*, 2010, **130**, 1258–1267.
46 R. Nandy and S. Sankararaman, *Beilstein J. Org. Chem.*, 2010, **6**, 992–1001 No 1112.
47 Y. Saito, A. Suzuki, K. Imai, N. Nemoto and I. Saito, *Tetrahedron Lett.*, 2010, **51**, 2606–2609.
48 S.-L. Wang, J.-M. Lin, S.-E. Shu and C.-Y. Chern, *J. Photochem. Photobiol., A*, 2010, **210**, 54–60.
49 J. R. Mansfield, K. W. Gossage, C. C. Hoyt and R. M. Levenson, *J. Biomed. Opt.*, 2005, **10**, 041207.
50 H. S. Basu, B. G. Feuerstein, D. A. Zarling, R. H. Shafer and L. J. Marton, *J. Biomol. Struct. Dyn.*, 1988, **6**, 299–309.
51 J. Nickol, M. Behe and G. Felsenfeld, *Proc. Natl. Acad. Sci. U. S. A.*, 1982, **79**, 1771–1775.
52 R. M. Santella, D. Grunberger, I. B. Weinstein and A. Rich, *Proc. Natl. Acad. Sci. U. S. A.*, 1981, **78**, 1451–1455.
53 T. E. Storr, A. G. Firth, K. Wilson, K. Darley, C. G. Baumann and I. J. S. Fairlamb, *Tetrahedron*, 2008, **64**, 6125–6137.
54 T. E. Storr, C. G. Baumann, R. J. Thatcher, S. De Ornellas, A. C. Whitwood and I. J. S. Fairlamb, *J. Org. Chem.*, 2009, **74**, 5810–5821.
55 *WO. Pat*, 2005123755, 2005.
56 *WO. Pat*, 2007091056, 2007.